https://doi.org/10.5194/egusphere-2026-1302
Preprint. Discussion started: 13 March 2026

Implementation and Evaluation of an Observation-Constrained Secondary Organic Aerosol Parameterization in MOZART–GOCART Chemistry in WRF-Chem

Rajmal Jat[1], Akash Sagar Vispute[1], Sachin D. Ghude[1], Rajesh Kumar[2], Vinayak Sinha[3], Baerbel Sinha[3], Gaurav Govardhan[1], Zhining Tao[4] Prafull P. Yadav[1,6], Sandeep Wagh[1], Sreyashi Debnath[1], Aditi Rathore[1], Madhavan Rajeevan[5]

[1]Indian Institute of Tropical Meteorology, Ministry of Earth Sciences, Pune, India

[2]NSF National Center for Atmospheric Research, Boulder, CO, US

[3]Indian Institute of Science Education and Research Mohali, Punjab, India

[4]Morgan State University, Baltimore, MD, USA

[5] National Centre for Earth Science Studies, Thiruvananthapuram, Kerala, India; Atria University, Bengaluru, India

[6] Dept. of Atmospheric and Space Sciences, Savitribai Phule Pune University, Pune, India

Correspondence: Rajmal Jat (rajmal.jat@tropmet.res.in) and Sachin D. Ghude (sachinghude@tropmet.res.in)

Abstract

A computationally inexpensive, observation-constrained parameterization for Secondary Organic Aerosols (SOA) formation is implemented and tested in the default MOZART–GOCART (MOZCART) chemical mechanism of the Weather Research and Forecasting model coupled with Chemistry (WRF-Chem). The outcomes were evaluated against hourly observations of SOA, Organic Aerosols (OA) and Fine particulate matter ($PM_{2.5}$) over Delhi during November 2024. Sector-specific Emissions ratios (ERs) derived from in-situ Volatile Organic Compounds (VOC) measurements in Delhi were used, with values of 77 ± 5, 130 ± 13, and 60 ± 9 ppbv VOC/ppmv CO for transportation, biomass burning, and industry-dominated plumes, respectively, to represent SOA formation from anthropogenic and open biomass burning precursors. The modified MOZCART scheme reproduces the temporal variability, with a monthly mean simulated concentration of 53 ± 24 µg/m^3 compared to an observed mean of 83 ± 43 µg/m^3 (RMSE = 58.2 µg/m^3; MFB = −0.53). Inclusion of SOA

https://doi.org/10.5194/egusphere-2026-1302
Preprint. Discussion started: 13 March 2026

parameterization substantially improves total organic aerosol (OA), increasing mean OA from 48 to 101 µg/m^3 and reducing normalized mean bias from −57.8% to −19.1%. $PM_{2.5}$ predictions also improve, with mean concentrations increasing from 151 to 203 µg m^{-3} and mean bias reduced by ~54%, alongside better reproduction peak pollution events. Intercomparison with other WRF-Chem mechanisms shows that MOZCART achieves SOA performance comparable to the more complex MOZART–MOSAIC scheme (RMSE = 58.2 vs. 54.8 µg/m^3) and substantially better than RADM2–SORGAM, while being ~5.3 times faster than MOZART–MOSAIC. These results demonstrate that the proposed simplified SOA parameterization provides an effective balance between accuracy and computational efficiency and can be effectively used in operational air quality forecasting over highly polluted urban regions like Delhi.

Keywords: Secondary Organic Aerosols, WRF-Chem, Parameterization, MOZCART, Emissions ratios

1 Introduction

Fine particulate matter ($PM_{2.5}$) in the atmosphere consists of both inorganic and carbonaceous aerosol species. Organic aerosols (OA) in carbonaceous aerosol contribute to a major fraction of fine particulate matter and lead to significant impacts on air quality and climate change (Forster et al., 2007; Jacobson et al., 2000; Tsimpidi et al., 2016; Hodzic et al., 2020). OA is a mixture of primary organic aerosols (POA), emitted directly from the source, and particulate matter formed through gas-to-particle conversion, either by condensation of POA oxidation products (Robinson et al., 2007) or through oxidation of volatile organic compounds (VOCs) and semi-volatile VOCs, termed as secondary organic aerosols (SOA) (Ervens et al., 2011). The emissions of POA and SOA precursor gases come from anthropogenic, biomass burning, and biogenic sources (Gouw et al., 2008; Sasidharan et al., 2023). The distribution of OA at spatial and temporal scales depends on the emission source strength, transportation and mixing in the atmosphere, chemical transformation, and removal in the atmosphere. The representation of formation mechanism and fate of OA in the atmosphere is highly uncertain in the atmospheric composition model (ACMs) and poses significant challenges, particularly the largest uncertainty sits in the mechanistic representation of SOA formation and its ageing

https://doi.org/10.5194/egusphere-2026-1302
Preprint. Discussion started: 13 March 2026

processes (Hodzic et al., 2016; Lannuque et al., 2018). The parametrization of SOA in CTMs is generally carried out using either the two-product schemes or the volatility basis set (VBS) scheme. The two-product scheme lumps the formation of low vapor pressure products formed through oxidation of organic gases by hydroxyl radical ($OH^{\cdot}$), Ozone (O_3) and nitrate radical ($NO_3^{\cdot}$) into two products. In this scheme, gas-to-particle conversion of low-pressure products follows the absorption process in organic mass, assuming the formation of quasi-ideal solution (Pankow, 1994). The VBS scheme is the advanced SOA parameterization scheme, which resolves the SOA formations using multiple volatility-resolved bins of condensable compounds (Donahue et al., 2006), and substantially improves the simulated SOA concentrations, providing improved agreement with observations (Hodzic et al., 2010; Shrivastava et al., 2011). However, VBS implementations are computationally expensive as they require tracking organic species across multiple volatility bins and aerosol size bins.

The formation of SOA in polluted airmasses has been estimated in measurement-based aerosol studies using the OA to effective CO (excluding background CO from total CO) ratio (de Gouw et al., 2005; De-Carlo et al., 2010), wherein CO is considered as quasi-inert tracer because it is nearly conserved against oxidation by OH at time scale of hours to days, which is relevant for SOA formation. The enhancement in this ratio in fresh and aged air masses is attributed to the formation of SOA due to anthropogenic and open biomass burning emissions and has been observed in multiple studies across the globe (de Gouw and Jimenez, 2009; DeCarlo et al., 2010; Cubison et al., 2011; Zhang et al., 2019; Oak et., 2022). Spracklen et al. (2011) and Hodzic and Jimenez (2011) developed a simplified parametrization to predict the SOA formation in the atmosphere based on these observed ratios in polluted plumes from anthropogenic and biomass burning sources. Spracklen et al. (2011) used the Global Model of Aerosol Processes (GLOMAP) to evaluate the simulated OA and SOA against the observed mass of these aerosols from multiple measurement locations. Spracklen et al. (2011) simulated SOA through lumped anthropogenic, lumped biomass burning, and biogenic VOCs and varied these sources to yield the best SOA estimates. Following the methodology of Spracklen et al. (2011), Hodzic and Jimenez (2011) developed a computationally inexpensive SOA parametrization in the CHIMERE regional chemistry model and compared against observations from the Mexico City metropolitan area during the Megacity Initiative: Local and Global Research Observations (MILAGRO) 2006 field experiment. They found that the SOA estimates for this parameterization were comparable to the simulated SOA from a

https://doi.org/10.5194/egusphere-2026-1302
Preprint. Discussion started: 13 March 2026

computationally expensive scheme by Robinson et al. (2007), which utilizes semi-volatile and intermediate volatility primary organic vapors for SOA predictions.

Air quality in Delhi has deteriorated markedly over recent decades, driven by rapid increases in population, urban expansion, vehicular activity, industrialization, and energy consumption, which have substantially enhanced anthropogenic emissions of particulate matter and gaseous co-pollutants (Ghude et al., 2008; Kumar et al., 2015; Gurjar et al., 2016). Episodic pollution during the post-monsoon and early winter period is strongly influenced by large-scale open burning of agricultural residues in the northwestern Indo-Gangetic Plain (Kumar, et al., 2021) particularly in Punjab and Haryana, which contributes significantly to regional pollutant loading and downwind transport into Delhi (Ambulkar et al., 2025; Govardhan et al., 2023 , Awasthi et al., 2024). These emissions, coupled with emissions from other anthropogenic sectors and unfavorable wintertime meteorology, further elevate the pollution loadings (Sengupta et al., 2022; Jat et al., 2021; Ghude et al., 2025). Consequently, Delhi experiences persistently high $PM_{2.5}$ levels, with the highest population-weighted annual mean among Indian megacities and substantial associated health and economic impacts (Pandey et al., 2021; Jat et al., 2024). To address the need for accurate and timely air quality forecasts over Delhi, institutions under the Ministry of Earth Sciences (MoES), including the Indian Institute of Tropical Meteorology (IITM) and the India Meteorological Department (IMD), in partnership with the U.S. National Science Foundation (NSF) National Center for Atmospheric Research (NCAR), have developed an advanced Air Quality Warning and Integrated Decision Support System for Emissions (AIRWISE) (Ghude et al., 2024; Jena et al., 2021; Yadav et al., 2025a). AIRWISE is a very high-resolution (400m × 400m) operational air quality forecasting system using the Weather Research and Forecasting model coupled with chemistry (WRF-Chem) at its core and incorporates three-dimensional Variational data assimilation using the community Gridpoint Statistical Interpolation (GSI) framework (Ghude et al., 2024; Kumar et al., 2020, Kumar et al., 2025; Yadav et al., 2025b).

This system uses the Model for Ozone and Related Chemical Tracers (MOZART) gas-phase chemical scheme coupled with the Georgia Tech/Goddard Global Ozone Chemistry Aerosol Radiation and Transport (GOCART) aerosol scheme (Emmons et al., 2010; Chin et al., 2000; Ginoux et al., 2001)), hereafter referred to as the MOZCART chemical mechanism. MOZCART is a bulk aerosol scheme, which is computationally very efficient and is hence being used in the AIRWISE system. However, this scheme doesn't include any secondary organic aerosol model within it and is therefore missing SOA, likely because explicit SOA

https://doi.org/10.5194/egusphere-2026-1302
Preprint. Discussion started: 13 March 2026

formation mechanisms (two-products scheme and VBS scheme) are computationally expensive. Therefore, in the present study, we implemented a computationally inexpensive, simplified SOA parameterization in the MOZCART chemical mechanism of WRF-Chem using in situ observations in Delhi and tested whether it can be used to simulate SOA reasonably.

2 Model Setup, Observations, and Parameterization.

2.1 Model Configurations:

The present study employs the WRF-Chem version 3.9.1 (Grell et al., 2005), with a horizontal grid spacing of 10 km × 10 km over a domain covering the Indian subcontinent. The model domain is divided into 420 grid points in the east–west direction and 372 grid points in the south–north direction. Gas-phase and aerosol chemistry in model are represented using the MOZCART scheme. Meteorological initial and boundary conditions are obtained from the National Centers for Environmental Prediction (NCEP) Final Analysis (FNL) data at 0.25° spatial and 6-hour temporal resolution. Anthropogenic emissions of trace gases and aerosols are taken from the Emissions Database for Global Atmospheric Research–Hemispheric Transport of Air Pollution (EDGAR-HTAP v2.2) inventory (Janssens-Maenhout et al., 2015) at a resolution of 0.1° × 0.1° for the base year 2010 and are scaled using factors provided by Venkataraman et al. (2018). Biomass burning emissions are obtained from the Fire INventory from NCAR (FINN) version 2.5 (Wiedinmyer et al., 2023), while for biogenic emissions, the Model of Emissions of Gases and Aerosols from Nature (MEGAN) (Guenther et al., 2006) is used to calculate those online within the model. Initial chemical and boundary conditions are provided by the global MOZART-4 model (Emmons et al., 2010). The simulation was conducted from 15th October – 30th November 2024, with model spin up of two weeks, i.e., the simulations for the period of October 15-31, 2024 are excluded from the analysis. Other Details of model setup are provided in the table 1.

Table 1. Configuration of options used in model setup

Physical Parameterization	Scheme used
PBL scheme	Mellor–Yamada–Nakanishi–Niino 2.5 (MYNN2.5) (Nakanishi and Niino (2006))
Microphysics scheme	Morrison double-moment (Morrison et al. (2009))
Longwave radiation scheme	Rapid Radiative Transfer Model for general circulation models (Iacono et al. 2008)
Shortwave radiation scheme	Rapid Radiative Transfer Model for general circulation models (Iacono et al. 2008)

https://doi.org/10.5194/egusphere-2026-1302
Preprint. Discussion started: 13 March 2026

Land surface scheme	Noah Land Surface Model (Chen and Dudhia, 2001)
Surface layer scheme	Monin–Obukhov (Janjic Eta) scheme (Janjić 2001)
Cumulus parameterization scheme	Grell–Freitas cumulus scheme (Grell and Freitas 2014)

2.2 Observational data and evaluation protocols:

Surface $PM_{2.5}$ data over Delhi used in this study were obtained from the air quality monitoring network of the Central Pollution Control Board (CPCB), India, for November 2024. A total of 39 monitoring stations were operational across Delhi during the study period, representing traffic, airport, urban, and suburban areas. The quality assurance and quality control (QA/QC) procedures followed by CPCB for these air quality monitoring stations are described at https://cpcb.nic.in/quality-assurance-quality-control/. Concentrations of secondary organic aerosol (SOA) in Delhi during November 2024 at the India Meteorological Department (IMD) site were estimated from organic aerosol (OA) mass spectra measurements of non-refractory fine particulate matter (NR-$PM_{2.5}$). The OA mass spectra were measured using a high-resolution time-of-flight aerosol mass spectrometer (HR-ToF-AMS), a state-of-the-art instrument for real-time, for characterization of non-refractory aerosol composition (DeCarlo et al., 2006; Canagaratna et al., 2007; Vispute et al., 2025). The instrument provides size-resolved chemical composition of aerosol species in NR-$PM_{2.5}$. Positive Matrix Factorization (PMF) analysis was applied to the OA mass spectra to apportion sources and to estimate SOA concentrations. In AMS applications, PMF-derived SOA represents an inferred oxygenated organic aerosol component rather than a direct independent instrumental measurement, and therefore carries uncertainty related to factor selection, rotational ambiguity, and possible mixing between primary and secondary organic aerosol components (Ulbrich et al., 2009; Crippa et al., 2014; Drosatou et al., 2019). AMS/ACSM studies show that such uncertainty is not fixed, but generally lies around ~10–40% for well-resolved major OOA factors, increasing to a factor of 2–3 when factor contributions are small (<10% of OA) or poorly separated (Drosatou et al., 2019; Fröhlich et al., 2015; Canonaco et al., 2021). Thus, the PMF-derived SOA used here should be regarded as an observationally constrained estimate.

The measurement of VOCs, used in estimating VOC/CO emission ratios, were taken during year 2022 at the Indian Meteorological Department site, located in central Delhi. The VOCs were measured using a new high sensitivity and high-mass resolution proton transfer reaction time-of-flight mass spectrometer (PTR-TOF-MS 10k). A total of 1126 peaks were detected

https://doi.org/10.5194/egusphere-2026-1302
Preprint. Discussion started: 13 March 2026

from the ambient air mass spectra, out of which 111 VOC compounds were confirmed and reported following the QA/QC procedures. More details about the measurements can be referred from Mishra et al. (2024). Model performance was evaluated by comparing hourly model predictions of SOA, OA and $PM_{2.5}$ with corresponding observations (SOA and OA from AMS observations, and $PM_{2.5}$ from CPCB monitoring network) using time-series analysis and standard statistical metrics, including Root Mean Square Error (RMSE), Mean Fractional Bias (MFB), Normalized Mean Bias (NMB), Mean Fractional Error (MFE), Mean Bias (MB), and Mean Absolute Error (MAE).

2.3 SOA Parameterization:

The default MOZCART chemistry is a bulk aerosol scheme with five major tropospheric aerosol species: black carbon, organic carbon, sulfate, dust, and sea salt (Chin et al., 2000; Ginoux et al., 2001). Owing to its relatively low computational cost, this scheme is widely used in operational air quality forecasting systems (Ghude et al., 2024). However, the default MOZCART configuration does not include secondary organic aerosol (SOA) formation processes, which are implemented in more detailed aerosol schemes (e.g., MOSAIC; Zaveri et al., 2008) within WRF-Chem. MOSAIC based schemes are computationally expensive. Here we present a computationally efficient first order SOA parametrization within MOZCART chemical mechanism of WRF-Chem.

At urban and regional scales, where anthropogenic and biomass burning emissions dominate, SOA formation via OH oxidation of VOCs occurs at the time scale of several hours to few days. At this time scale, carbon monoxide (CO) remains approximately conserved with respect to OH oxidation (DeCarlo et al., 2010). Consequently, CO can be treated as an approximately conserved tracer, and SOA can be estimated using the ratio of organic aerosol to excess CO (after subtraction of background CO), where an increase in this ratio is attributed to SOA formation (Hodzic and Jimenez, 2011). The SOA to excess CO ratio is therefore assumed to be approximately equal to the VOC to CO emission ratio (ER) in the aged polluted airmass. Following the basics of approaches used in previous studies (DeCarlo et al., 2010; Hodzic and Jimenez, 2011; Spracklen et al., 2011), SOA formation from anthropogenic and biomass burning precursors is parameterized in MOZCART chemical mechanism in the present study using VOC/CO emission ratios (ERs) derived from in-situ measurements in Delhi. The gas-

https://doi.org/10.5194/egusphere-2026-1302
Preprint. Discussion started: 13 March 2026

phase chemistry of conversion of semi-volatile or intermediate volatile organic products to SOA through oxidation is accounted and lumped together in this approach. The emissions of VOC from anthropogenic sources and open biomass burning are estimated first which undergo oxidation to form SOA attributed to these sources. The emissions of anthropogenic and biomass burning VOCs are estimated using the VOC to CO emissions ratio (ERs) based upon the in-situ VOC measurements in Delhi conducted in the same months in 2022. Nearly 111 VOCs were measured during the post-monsoon period in Delhi (Mishra et al., 2024). Through the source apportionment (Awasthi et al., 2024) and multiple axis regression analysis, the VOC/CO ERs were estimated for different plumes dominated by particular emissions sectors (Figure 1). For the plumes dominated by the transportation sectors, the ERs was 77±5 ppbv VOC/ppmv CO. The plumes with more than 60 % of VOC burden from transportation sectors were considered here, while other sources contribute less than 20 %. Likewise, the ERs for open biomass burning dominated VOC plumes is estimated to be 130±13 ppbv VOC/ppmv CO , with more than 60 % VOC loading from the biomass burning sector, and the rest of the sectors were contributing not more than 20 %. For the industry sources, the ERs were 60±9 ppbv VOC/ppmv CO, where more than 40 % VOC plumes were from industry-dominated areas. We considered ERs of 60±9 ppbv VOC/ppmv CO for other emissions sectors. The emitted surrogate VOC from anthropogenic sources (Industrial (VOC_{IND}), Transportation (VOC_{TRA}), Other Sectors (VOC_{OTHR})) and open Biomass Burning (VOC_{BB}) are added to total VOC emissions (VOC_{ABB}) which undergo photochemical oxidation with hydroxyl radical ($OH^{\cdot}$) to form SOA_{ABB} in aerosol phase with 100 % mass yield. Following reactions, with reaction rates are utilized and added into MOZCART chemistry. This approach was followed by Hodzic and Jimenez, 2011 and implemented these reactions in the CHIMERE chemical transport model.

$$VOC_{ABB} + OH^{-1} \rightarrow SOA_{ABB} \quad (r = 1.25 \times 10^{-11}\ {}^{cm^3}/_{molecules - seconds}) \qquad (1)$$

https://doi.org/10.5194/egusphere-2026-1302
Preprint. Discussion started: 13 March 2026

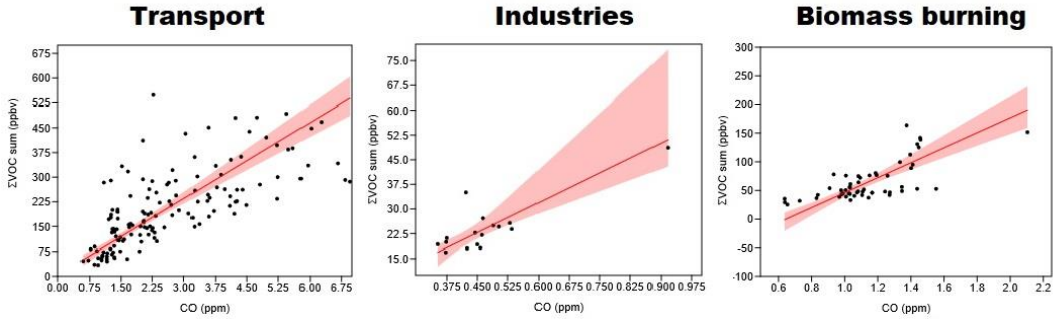

Figure 1: RMA analysis of VOC measurement for the sector dominated pollution plumes for estimating VOC/CO Emissions Ratios (ER).

Further, to understand the contributions from different source sectors to the simulated SOA_{ABB} yield, we have added four tagged tracers SOA species representing contributions from Industrial (SOA_{IND}), Transportation (SOA_{TRA}), Biomass burning (SOA_{BB}) and Other sector (SOA_{OTHR}). Like the regular SOA species, these tracer species undergo all physical and chemical processes, including emissions, transport, transformation, and deposition, except that they do not provide any direct or indirect feedback to the model, as such feedbacks are accounted for by the regular SOA_{ABB} species. The following parameterization equation is used for the tagged tracer species to estimate their contributions to SOA_{ABB}.

$$VOC_{tracer} + OH^{-1} \rightarrow SOA_{tracer} + OH^{-1} \ (r = 1.25 \times 10^{-11} \ {cm^3}/{molecules - seconds}) \quad (2)$$

2.4 SOA sensitivity:

The simulated SOA based on the newly developed parameterization in the MOZCART chemistry scheme is also compared with results from more complex gas–aerosol chemical mechanisms available in the WRF-Chem model, which are generally not suitable for operational forecasting due to their high computational cost. Two chemical mechanisms were selected for comparison: (i) the Second Generation Regional Acid Deposition Model gas-phase mechanism coupled with the Modal Aerosol Dynamics Model for Europe and Secondary

https://doi.org/10.5194/egusphere-2026-1302
Preprint. Discussion started: 13 March 2026

Organic Aerosol Model (RADM2–MADE/SORGAM) (Stockwell et al., 1990; Ackermann et al., 1998; Schell et al., 2001), and (ii) the Model for Ozone and Related Chemical Tracers gas-phase mechanism coupled with the Model for Simulating Aerosol Interactions and Chemistry (MOZART–MOSAIC). These mechanisms adopt different approaches for SOA parameterization.

The MOZART–MOSAIC mechanism uses a sectional approach to represent particle size distributions across different size bins. In this study, a 4-bin configuration is employed. SOA formation in MOZART–MOSAIC is parameterized using the volatility basis set (VBS) framework described by Knote et al. (2015), which considers five volatility bins with effective saturation concentrations of 10^{-4}, 1, 10, 100, and 1000 µg/m3. The extent of SOA formation varies across low and high NO_x regimes during oxidation of precursors by hydroxyl radicals (OH). The RADM2–MADE/SORGAM mechanism employs a modal aerosol scheme that represents aerosol size distributions using lognormal modes (Aitken, accumulation, and coarse modes). The SORGAM module parameterizes SOA formation using a two-product approach. The VOCs get oxidized first through photochemical oxidation into low-volatility organic products, which interact and condense into practical phase. The gas to particle partitioning of these compounds is simulated as an absorption process into the organic mass on the aerosol particle, assuming the formation of a quasi-ideal solution (Schell et al., 2001).

Two simulations were conducted, one using MOZART–MOSAIC and the other using RADM2–MADE/SORGAM. Both simulations were performed for the period 1–30 November 2024, preceded by a two-week spin-up period from 15 to 31 October 2024. The simulated SOA from the updated MOZCART, MOZART–MOSAIC, and RADM2–MADE/SORGAM is compared with measured SOA concentrations over Delhi.

3. Results and discussion

3.1 Performance evaluation of SOA parametrization:

The model-predicted hourly SOA concentrations were compared with hourly observed SOA in non-refractory $PM_{2.5}$ (NR-$PM_{2.5}$; particulate matter with aerodynamic diameter ≤ 2.5 µm) over Delhi during November 2024, as shown in figure 2. The temporal evolution indicates that the SOA parameterization reasonably captures the observed variability. During 9–12 November,

https://doi.org/10.5194/egusphere-2026-1302
Preprint. Discussion started: 13 March 2026

peaks in observed SOA are well synchronized with those in the simulated SOA. For example, on 11th November, observed SOA increased from 65 μg/m^3 to 97 μg/m^3, while simulated SOA increased from 78 μg/m^3 to 94 μg/m^3. During this period, the model reproduces SOA well, with a mean simulated concentration of 84 μg/m^3 compared to a mean observed concentration of 80 μg/m^3. Daytime and nighttime periods are indicated by white and grey shading, respectively, in figure 2a. The model also reproduces the photochemical production of SOA during late morning to early afternoon hours (~09:00–13:00 IST), as shown in figure 2b. However, the pattern of diurnal SOA does not match well between observation and simulation, which could be attributed to uncertainties in simulating the diurnal evolution of boundary layer height, in the diurnal variation of emissions, and in emission inventory, as well as the assumption that SOA production occurs only through oxidation by OH radicals. It should also be noted that aged biomass-burning emissions can contribute substantially to oxygenated OA factors in AMS-PMF analysis; therefore, part of the PMF-derived SOA enhancement during 9–12 November may reflect biomass-burning-influenced secondary OA, rather than exclusively secondary OA from non-biomass-burning sources (Aiken et al., 2010; Cubison et al., 2011).

During 13th–19th November, observed SOA concentrations were substantially higher, with a mean value of approximately 133 μg/m^3 and peak concentrations reaching up to 223 μg/m^3. During this period, SOA levels were significantly underestimated by the parameterization, with a mean simulated SOA of approximately 47 μg/m^3. To investigate the cause of this discrepancy, biomass burning–related organic aerosol (OA) concentrations from observations were analyzed (Figure 3). The observed biomass burning OA exhibited very high concentrations, exceeding 300 μg/m^3, and closely followed the temporal pattern of elevated observed SOA during this period. This indicates that the enhanced SOA loading over Delhi during 13–19 November was primarily driven by emissions from open biomass burning in northwestern India. Furthermore, dense fog and haze conditions prevailed over northwestern India during this period, which limited the satellite detection of active fires, particularly over Punjab and Haryana (Figure S2). As a result, fire counts and associated biomass burning emissions were underestimated in the model, leading to significantly lower simulated SOA concentrations. This underestimation is also evident in the SOA time series showing contributions from the open biomass burning sector.

As discussed in the previous section, SOA parameterization has been implemented separately for different source sectors according to dominated pollution plume analysis. To further examine the evolution of SOA in the model, the contributions from individual source sectors

https://doi.org/10.5194/egusphere-2026-1302
Preprint. Discussion started: 13 March 2026

to the simulated total SOA were also analyzed (Figure 2a). The mean sectoral contributions during November 2024 from the transportation, industrial, biomass burning, and other sectors were 11 μg/m^3, 7 μg/m^3, 15 μg/m^3, and 20 μg/m^3, respectively (Figure S1). The temporal variations and peak values of biomass burning–derived SOA show reasonable agreement with the observed SOA trends. During peak SOA episodes, biomass burning was the dominant contributor among all sectors, with contributions reaching up to 42 μg/m^3, thereby reproducing the timing of observed SOA peaks, although with lower magnitudes due to underestimated fire emissions during the peak biomass burning period. The statistical evaluation (Table 2) indicates that the mean simulated and observed SOA concentrations during November 2024 were 53 μg/m^3 and 83 μg/m^3, respectively, corresponding to a mean fractional bias (MFB) of −0.53.

https://doi.org/10.5194/egusphere-2026-1302
Preprint. Discussion started: 13 March 2026

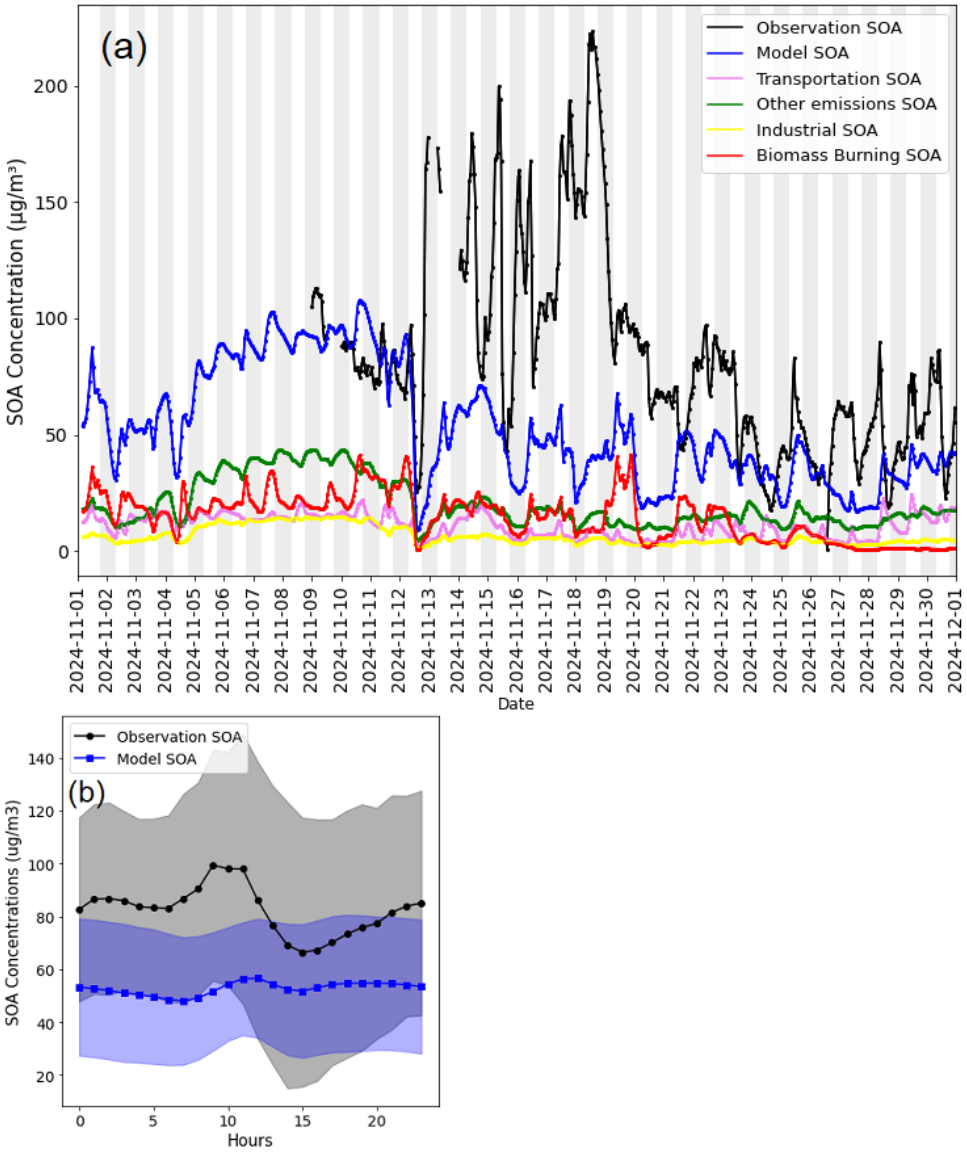

Figure 2: (a) The Comparison of simulated hourly SOA concentrations from modified MOZCART chemistry against the observed SOA in Delhi during November 2024. Contributions from different source sectors to total simulated SOA are also presented. (b) mean diurnal variation in simulated and Observed SOA in Delhi.

As SOA is added in MOZCART chemical mechanism, we further analyzed changes in the simulated total organic aerosol (OA) by comparing model predictions with observed OA

https://doi.org/10.5194/egusphere-2026-1302
Preprint. Discussion started: 13 March 2026

concentrations over Delhi (Figure 3). For this purpose, two modeled OA time series—one without SOA and one with SOA parameterization—were compared against observed OA to assess the impact of the added SOA scheme. The default model configuration without SOA shows substantial underestimation of observed OA, with a mean simulated OA concentration of 48 μg/m^3 compared to an observed mean of 117 μg/m^3 during the study period. In contrast, inclusion of SOA parameterization leads to a significant improvement in OA predictions, with the simulated hourly variability more closely following observations and a mean OA concentration of 101 μg/m^3. However, during the peak pollution episode from 13–18 November 2024, OA remains substantially underestimated, primarily due to the underestimated fire counts in satellite observations, as discussed earlier. For example, during this period, the mean simulated OA was 90 μg/m^3, whereas the observed mean was 197 μg/m^3, indicating an underestimation of nearly 50%. Model performance statistics are summarized in Table 2. The metrics indicate that inclusion of SOA in the MOZCART chemistry scheme results in substantial reductions in bias. For instance, the NMB (MFB) improve from −57.8% (−0.63) to −19.1% (−0.04). Similarly, the RMSE (MAE) decrease to 90 μg/m^3 (55.9 μg/m^3), representing improvements of 19 μg/m^3(15.9 μg/m^3) compared to the simulation without SOA.

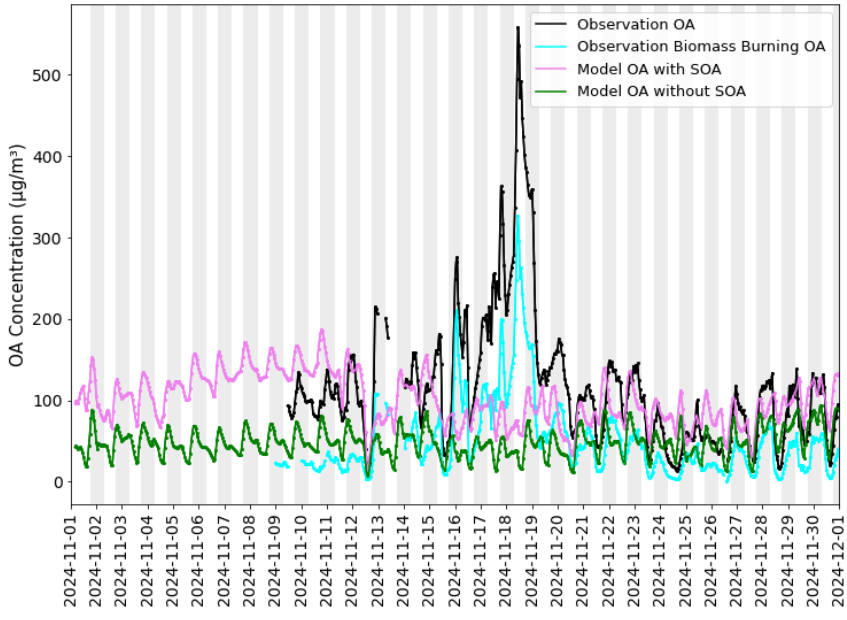

Figure 3: The Comparison of simulated OA concentrations from modified MOZCART chemistry and default MOZCART chemistry against the observed OA in Delhi during November 2024. OA from biomass burning in observations is also presented.

https://doi.org/10.5194/egusphere-2026-1302
Preprint. Discussion started: 13 March 2026

To assess the impact of SOA parameterization in the MOZCART chemical mechanism on predicted $PM_{2.5}$, model performance was evaluated for two cases: with and without SOA parameterization. Hourly comparisons of predicted $PM_{2.5}$ for both cases against observed $PM_{2.5}$ over Delhi are shown in figure 4. The hourly time series indicates that the underestimation in the default configuration is reduced when SOA parameterization is included, and the gap between observed and simulated $PM_{2.5}$ is considerably narrowed. Most of the observed $PM_{2.5}$ peaks are well captured by the model when SOA is included. Performance statistics are summarized in Table 2. The mean simulated $PM_{2.5}$ concentration during the study period increases from 151 $\mu g/m^3$ to 203 $\mu g/m^3$ with SOA parameterization, reducing MB and NMB by 54% (from -98.2 to -45.5 $\mu g/m^3$) and 53% (from -39.4% to -18.3%), respectively. Metrics that account for both systematic and random errors also indicate overall improvement. For example, the RMSE and MFE decrease from 163 $\mu g/m^3$ and 0.5 to 144 $\mu g/m^3$ and 0.4, respectively. At the mean diurnal scale (Figure 4b), the magnitude of the $PM_{2.5}$ diurnal variation is improved in the simulation with SOA parameterization, except for an overestimation during the evening hours (17-20 hrs. IST), and biases during both daytime and nighttime are reduced. Overall, inclusion of SOA parameterization improves $PM_{2.5}$ predictions; however, uncertainties remain due to uncertainties in emissions, meteorological fields, atmospheric processes, and numerical approximations.

https://doi.org/10.5194/egusphere-2026-1302
Preprint. Discussion started: 13 March 2026

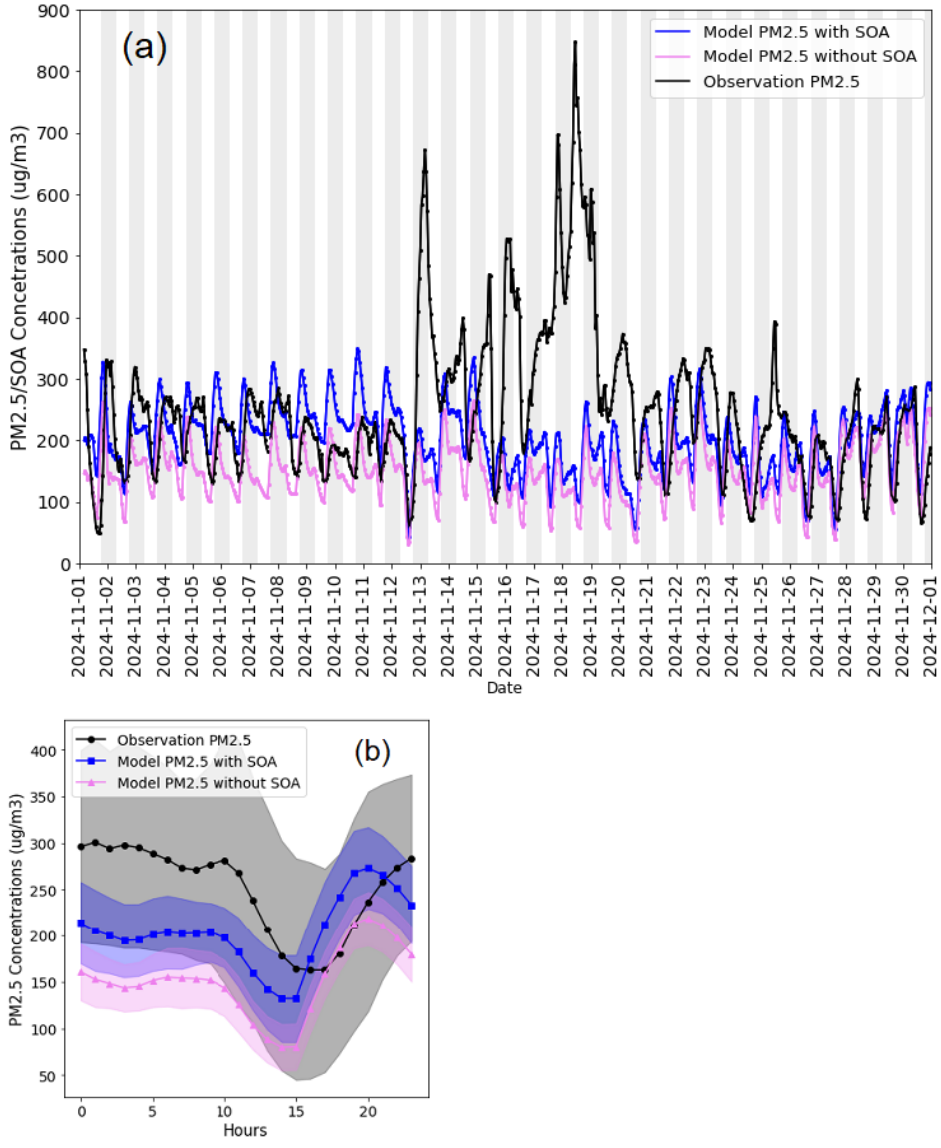

Figure 4: (a) The Comparison of simulated hourly $PM_{2.5}$ concentrations from modified MOZCART chemistry and default MOZCART chemistry against the observed SOA in Delhi during November 2024. (b) Mean diurnal variation in simulated and Observed $PM_{2.5}$ in Delhi.

https://doi.org/10.5194/egusphere-2026-1302
Preprint. Discussion started: 13 March 2026

Table 2: Statistical analysis of SOA and PM2.5 predictions during November 2024.

	November 2024							
	Predicted ($\mu g/m^3$)	**Observed** ($\mu g/m^3$)	**RMSE** ($\mu g/m^3$)	**MFB**	**NMB (%)**	**MFE**	**MB** ($\mu g/m^3$)	**MAE** ($\mu g/m^3$)
SOA (µg/m3)	53 ± 24	83 ± 43	58.2	-0.53	-45.8	0.6	-38	41.5
PM2.5 (µg/m3) (Without SOA)	151 ± 47	249 ± 120	163	-0.42	-39.4	0.5	-98.2	113.4
PM2.5 (µg/m3) (With SOA)	203 ± 55		144	-0.13	-18.3	0.4	-45.5	96
OA (µg/m3) (Without SOA)	48 ± 17	117 ± 83	109	-0.63	-57.8	0.7	-67.5	71.8
OA (µg/m3) (With SOA)	101 ± 31		90	-0.04	-19.1	0.5	-22.2	55.9

3.2 Spatial Distribution of SOA:

The spatial distribution of mean SOA during November 2024 is shown in figure 5. SOA concentrations over the Indo-Gangetic Plain (IGP) range from 50 to 85 $\mu g/m^3$, with higher concentrations over the downwind regions of the IGP under the prevailing northwesterly winds. Over central India, SOA concentrations are lower, in the range of approximately 40–50 $\mu g/m^3$. The photochemical production of SOA in the emission plume and its regional transport is reproduced well in the model and nearly ~10-30 $\mu g/m^3$ SOA concentrations were simulated over the oceanic regions. To examine the contributions of different source sectors to total simulated SOA, spatial distributions of sectoral SOA contributions are also shown (Figure 5b–e). Contributions from the transportation and industrial sectors are approximately 10–15 $\mu g/m^3$ over the IGP. SOA contributions from other sectors (energy and residential) range from ~25 to 40 $\mu g/m^3$ over the IGP, with higher values over Uttar Pradesh and Bihar, where clustering of power plants (Jat et al., 2024) are prevalent. Contributions from the biomass burning sector are dominant over Punjab and Haryana states, with mean SOA concentrations of about 25–30 $\mu g/m^3$ over these regions. As noted earlier in the discussion of temporal SOA variations over Delhi during November 2024, satellite-based fire detections were substantially underestimated during mid-November due to dense fog conditions. Consequently, fire counts and associated

https://doi.org/10.5194/egusphere-2026-1302
Preprint. Discussion started: 13 March 2026

biomass burning emissions were underestimated in the model, leading to lower simulated SOA formation from open biomass burning over northwestern India. As a result, the modeled mean SOA over Punjab and Haryana is approximately 50 μg/m^3. To further investigate this issue, we analyzed fire-related CO emissions for November 2023 and November 2024 and found that CO emissions over Punjab in November 2024 were 40–70% lower than those in November 2023, providing clear evidence of underestimation in detected fire activity due to foggy conditions in mid-November 2024 (Figure S3).

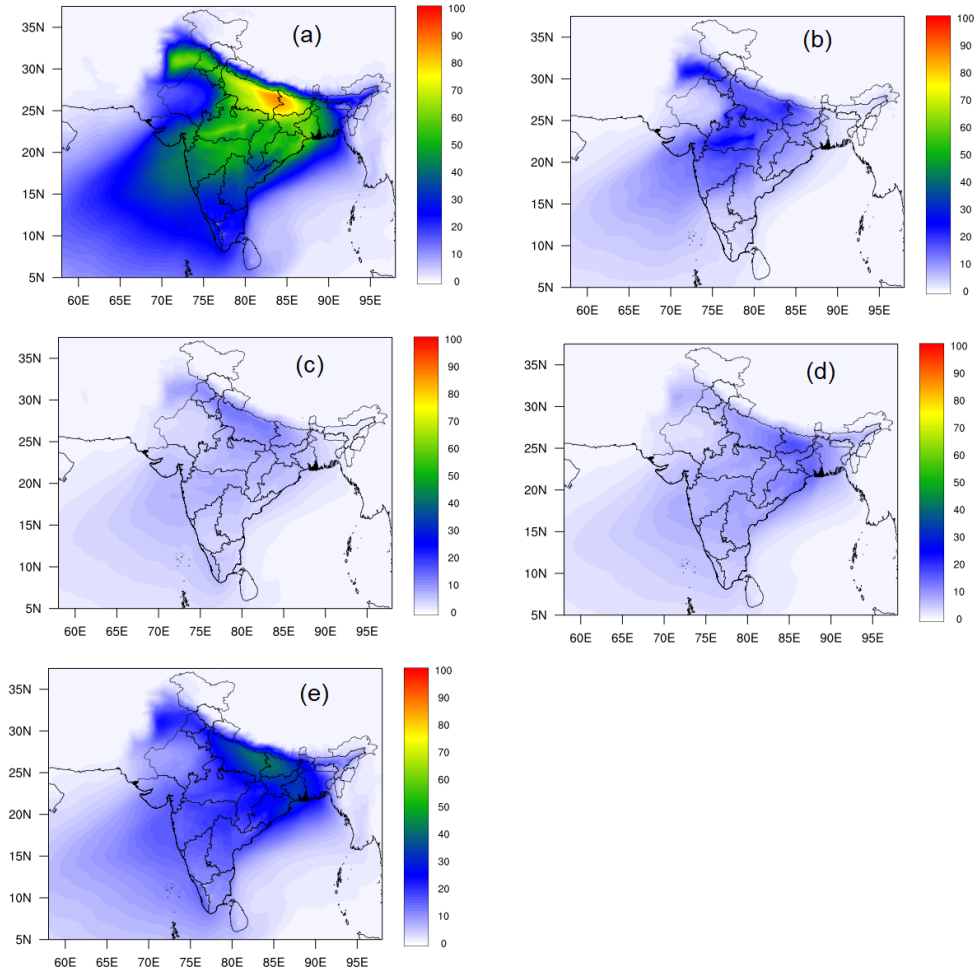

Figure 5: The Spatial distribution of mean SOA (μg/m^3) (a) and contribution to SOA from Biomass burning (b), Transportation (c), Industrial (d) and other sectors (e) during November 2024.

https://doi.org/10.5194/egusphere-2026-1302
Preprint. Discussion started: 13 March 2026

3.3 Comparison of SOA formation in MOZCART with different chemical schemes:

The simulated SOA over Delhi obtained using the newly developed parameterization in the MOZCART chemistry scheme is also compared with SOA simulated using other chemical mechanisms in WRF-Chem that include built-in SOA parameterizations (Figure 6 and Table 3). The mean simulated SOA concentration over Delhi from MOZCART is 53 μg/m^3, which is comparable to that from MOZART–MOSAIC (62 μg/m^3), whereas RADM2–SORGAM produces substantially lower SOA (27 μg/m^3). Statistical evaluation against observed SOA (Table 3) indicates that the performances of MOZCART and MOZART–MOSAIC are comparable, while the RADM2–SORGAM mechanism shows poorer performance. For example, the RMSE (NMB) values for MOZCART and MOZART–MOSAIC are 58.2 μg/m^3 (−45.8%) and 54.8 μg/m3 (−33%), respectively, whereas RADM2–SORGAM yields an RMSE of 70 μg/m^3 and an NMB of −65.5%. These results suggest that the simplified SOA parameterization implemented in MOZCART reproduces SOA reasonably well, outperforming RADM2–SORGAM and approaching the performance of the more complex MOZART–MOSAIC scheme. The good performance of MOZART–MOSAIC is expected, as it employs a volatility basis set (VBS) approach that accounts for SOA formation under both high- and low-NO_x regimes, includes five volatility bins with different saturation concentrations, and represents functionalization (ageing) of organic aerosols through OH oxidation. These detailed treatments enable more realistic SOA representation but at a substantially higher computational cost as MOZART–MOSAIC keeps track of the organic and aerosol species in 5 volatility bins and 4 particle size bins. To assess computational efficiency, the runtime of each chemistry scheme was analyzed for the study period. MOZCART was approximately 5.3 times faster than MOZART–MOSAIC and about 2.3 times faster than RADM2–SORGAM, corresponding to runtime reductions of approximately 81% and 57%, respectively. Although MOZART–MOSAIC provides the most detailed and accurate SOA representation, its high computational cost limits its applicability for operational air quality forecasting. In contrast, MOZCART, with the simplified SOA parameterization, achieves comparable statistical performance while being computationally efficient, making it more suitable for operational forecasting applications while still reproducing SOA reasonably well.

https://doi.org/10.5194/egusphere-2026-1302
Preprint. Discussion started: 13 March 2026

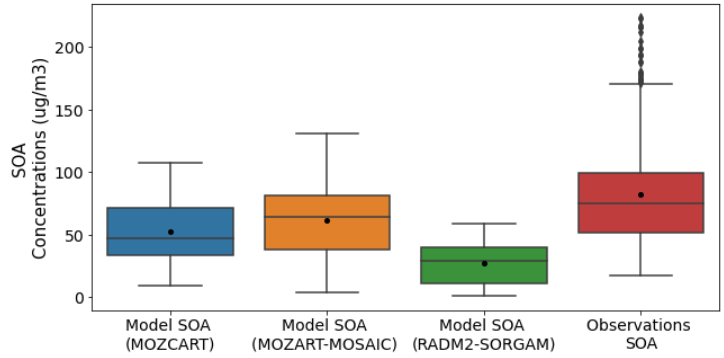

Figure 6: Comparison of simulated SOA from parameterization in MOZCART chemical mechanisms with the other chemical mechanisms in WRF-Chem.

Table 3: Statistical analysis of simulated SOA (µg/m^3) by different chemical mechanisms in Delhi during November 2024.

Chemical Mechanisms	Predicted	Observed	RMSE (µg/m3)	MFB	NMB (%)	MFE	MB (µg/m3)	MAE (µg/m3)
MOZCART	53 ± 24	83 ± 43	58.2	-0.53	-45.8	0.6	-38	41.5
MOZART-MOSAIC	62 ± 27		54.8	-0.36	-33	0.5	-27.4	37.7
RADM2-SORGAM	27 ± 15		70	-0.93	-65.5	0.9	-54.4	54.8

4. Future outlook and limitations of present study

The simplified SOA parameterization implemented in the present study in MOZCART chemistry assumes 100 % SOA production by oxidation with OH radicals only. It is noted that the mean diurnal variation in SOA was not reproduced well with observation peak lagging by 3 hours behind the modelled peak. This mismatch may partially be improved by considering other oxidant like ozone which would then attribute the part of SOA production by oxidation with ozone, keeping partitioning of yields between OH and ozone with in the experimentally observed range. Chamber studies demonstrated substantial contributions to SOA yield by ozonolysis of alkenes, isoprene and monoterpenes (Harvey and Petrucci, 2015). Under high-

https://doi.org/10.5194/egusphere-2026-1302
Preprint. Discussion started: 13 March 2026

NO_x conditions, SOA yields from OH oxidation (20–40%) are generally comparable to those from other oxidants (Ng et al., 2007; Hildebrandt et al., 2009). Similarly, SOA aging upon addition of nitrate radicals through night time chemistry (Ramasamy et al., 2019), also highlight the need of adding some simple proxy of adding nitrate in the MOZCART chemistry. To add the nitrate aerosols, future studies are required on developing a computationally faster parametrization of nitrate chemistry in MOZCART, which is currently unavailable in the default MOZCART chemistry in WRF-Chem. In addition to preceding improvements SOA parameterization, biases may partially be improved constraining the uncertainty in emissions. Open waste burning primary emissions were missing in the emission inventory used here, and a recent study reported that it accounts for nearly a quarter of the total PM2.5 emissions (~1000 Gg/year) in the year 2021 in India, which can contribute additional VOCs to biomass burning (Chaudhary et al., 2021). Likewise, VOC emissions estimates from the transportation sector in India in year 2015, based upon India-based measured emission factors, shows over estimation of VOCs in EDGARv4.3.2 and REASv.2.1 (Hakkim et al., 2021). Overall, further studies by incorporating emissions from missing sectors alongside improved SOA parametrization with additional oxidants and nitrate chemistry is expected to reduce biases in both the mean diurnal cycle and absolute magnitude of simulated SOA and $PM_{2.5}$.

5. Conclusions

In this study, a simplified and computationally efficient SOA parameterization based on VOC-to-CO emission ratios (ERs) derived from in-situ VOC observations in Delhi was implemented in the MOZART–GOCART (MOZCART) chemistry scheme within WRF-Chem. The simulated SOA from this parameterization and its impact on simulated OA and $PM_{2.5}$ concentration were evaluated over Delhi by comparison with observations. In addition, SOA simulated using this new parameterization was intercompared with other chemical schemes in WRF-Chem having different built in SOA models within their framework. The evaluation was conducted for November 2024, a period strongly influenced by open biomass burning in northwestern India. Sector-specific ERs derived from VOC measurements conducted during November 2022 at the IMD supersite in Delhi were 130±13 ppbv VOC/ppmv CO for biomass burning dominated plumes, 60±9 ppbv VOC/ppmv CO for industry dominated plumes, and ppbv VOC/ppmv CO for transportation dominated plumes.

https://doi.org/10.5194/egusphere-2026-1302
Preprint. Discussion started: 13 March 2026

The implemented simplified SOA parameterization in MOZCART successfully captures the temporal evolution of PMF-derived observed SOA over Delhi, with monthly mean concentrations of 53 ± 24 μg/m^3 compared to observed 83 ± 43 μg/m^3, an RMSE of 58.2 μg/m^3, and a MFB of −0.53. Biomass burning emerges as the dominant contributor to high SOA episodes, with modeled peak timings consistent with observations, although magnitudes are underestimated likely due to uncertainties in fire emission estimates. The strong underprediction was noted during 13th–19th November which was primarily attributed to underestimation of biomass burning emissions caused by limited satellite fire detection under persistent fogy conditions. Despite these limitations, parameterization provides a computationally efficient approach that reasonably captures SOA variability and is suitable for inclusion in operational air quality forecasting systems. Incorporation of the SOA parameterization in MOZCART leads to substantial improvements of simulated OA and $PM_{2.5}$ concentrations. For instance, incorporating SOA reduces NMB from −57.8% to −19.1% and RMSE by ~19 μg/m^3 in OA compared to the default configuration without SOA. Likewise, $PM_{2.5}$ prediction also improved with increasing mean concentrations by ~35% and reducing mean bias by ~54%, with RMSE decreasing from 163 μg/m^3 to 144 μg/m^3 and mean fractional error from 0.5 to 0.4. Intercomparison with other WRF-Chem chemistry mechanisms indicates that MOZCART with the simplified SOA parameterization achieves SOA prediction accuracy comparable to the more complex MOZART–MOSAIC scheme and substantially better than RADM2–SORGAM, with RMSE and NMB values of 58.2 μg/m3 and −45.8%, respectively. At the same time, MOZCART is approximately 5.3 times faster than MOZART–MOSAIC and 2.3 times faster than RADM2–SORGAM, corresponding to runtime reductions of about 81% and 57%, respectively. Although MOZART–MOSAIC provides the most detailed representation of SOA through a volatility basis set (VBS) framework, the simplified MOZCART approach offers an optimal balance between accuracy and computational efficiency for regional operational applications. Overall, these findings demonstrate that emission-ratio based SOA parameterizations constrained by local observations provide an effective and practical pathway for improving aerosol predictions in operational air quality forecasting systems over highly polluted urban regions.

https://doi.org/10.5194/egusphere-2026-1302
Preprint. Discussion started: 13 March 2026

Code and data availability: The model code, post-processing codes, and data used in this study are available at https://doi.org/10.5281/zenodo.18937872 (Jat et al., 2026). The model output is archived on the IITM high-performance computing facility and may be obtained upon request from the corresponding authors.

Author contributions: Conceptualization and Methodology: RJ, SDG, GG, RK, ZT, VS, BS. Data curation: ASV, VS, BS. Analysis and result interpretation: RJ, ASV, SDG, VS, BS, RK, PPY, GG. Writing (original draft preparation): RJ. Writing (review and editing): All authors. Supervision: SDG, GG, MR.

Competing interests: The authors declare that they have no conflict of interest.

Acknowledgements: We acknowledge the high-performance computing support provided by the Arka facility at the Indian Institute of Tropical Meteorology (IITM), Pune. We also acknowledge the use of surface $PM_{2.5}$ data from the air quality monitoring network of the Central Pollution Control Board (CPCB), India. The authors are grateful to the Director of the IITM, Pune for his support and encouragement. The work is partially supported by the Ministry of Earth Sciences (MOES), Government of India, to support the RASAGAM (Realtime Ambient Source Apportionment of Gases and Aerosol for Mitigation) project (grant no. MOES/16/06/2018-RDEAS).

References

Ackermann, I.J., Hass, H., Memmesheimer, M., Ebel, A., Binkowski, F.S., and Shankar, U.: Modal aerosol dynamics model for Europe: development and first applications, Atmos. Environ., 32, 2981–2999. https://doi.org/10.1016/S1352-2310(98)00006-5, 1998.

Aiken, A. C., Salcedo, D., Cubison, M. J., Huffman, J. A., DeCarlo, P. F., Ulbrich, I. M., Docherty, K. S., Sueper, D., Kimmel, J. R., Worsnop, D. R., Trimborn, A., Northway, M., Stone, E. A., Schauer, J. J., Volkamer, R. M., Fortner, E., de Foy, B., Wang, J., Laskin, A., Shutthanandan, V., Zheng, J., Zhang, R., Gaffney, J., Marley, N. A., Paredes-Miranda, G., Arnott, W. P., Molina, L. T., Sosa, G., and Jimenez, J. L.: Mexico City aerosol analysis during MILAGRO using high resolution aerosol mass spectrometry at the urban supersite (T0) – Part 1: Fine particle composition and organic source apportionment, Atmos. Chem. Phys., 9, 6633–6653, https://doi.org/10.5194/acp-9-6633-2009, 2009.

https://doi.org/10.5194/egusphere-2026-1302
Preprint. Discussion started: 13 March 2026

Ambulkar, R., Govardhan, G., Gavhale, S., Kalita, G., Pande, C., Jat, R., Kulkarni, S., Khare, M., Attri, S.D. and Ghude, S.D.: Crop residue burning in north-western India: Emission estimation and uncertainty quantification, J. Geophys. Res. Atmos, 130, e2024JD042198, https://doi.org/10.1029/2024JD042198, 2025.

Awasthi, A., Sinha, B., Hakkim, H., Mishra, S., Mummidivarapu, V., Singh, G., Ghude, S. D., Soni, V. K., Nigam, N., Sinha, V., and Rajeevan, M.N.: Biomass-burning sources control ambient particulate matter, but traffic and industrial sources control volatile organic compound (VOC) emissions and secondary-pollutant formation during extreme pollution events in Delhi, Atmos. Chem. Phys., 24, 10279–10304, https://doi.org/10.5194/acp-24-10279-2024, 2024.

Canagaratna, M. R., Jayne, J. T., Jimenez, J. L., Allan, J. D., Alfarra, M. R., Zhang, Q., Onasch, T. B., Drewnick, F., Coe, H., Middlebrook, A., Delia, A., Williams, L. R., Trimborn, A. M., Northway, M. J., DeCarlo, P. F., Kolb, C. E., Davidovits, P., and Worsnop, D. R.: Chemical and microphysical characterization of ambient aerosols with the Aerodyne aerosol mass spectrometer, Mass Spectrom. Rev., 26, 185–222. https://doi.org/10.1002/mas.20115, 2007.

Canonaco, F., Tobler, A., Chen, G., Sosedova, Y., Slowik, J. G., Bozzetti, C., Daellenbach, K. R., El Haddad, I., Crippa, M., Huang, R.-J., Furger, M., Baltensperger, U., and Prévôt, A. S. H.: A new method for long-term source apportionment with time-dependent factor profiles and uncertainty assessment using SoFi Pro: application to 1 year of organic aerosol data, Atmos. Meas. Tech., 14, 923–943, https://doi.org/10.5194/amt-14-923-2021, 2021.

Chaudhary, P., Garg, S., George, T., Shabin, M., Saha, S., Subodh, S. and Sinha, B.: Underreporting and open burning–the two largest challenges for sustainable waste management in India, Resour. Conserv. Recycl., 175, 105865, https://doi.org/10.1016/j.resconrec.2021.105865, 2021.

Chen, F., and Dudhia, J.: Coupling an advanced land surface–hydrology model with the penn state–NCAR MM5 modeling system. Part I: model implementation and sensitivity, Mon. Weather Rev., 129, 569–585, https://doi.org/10.1175/1520-0493(2001)129%3C0569:CAALSH%3E2.0.CO;2, 2001.

Chin, M., Rood, R.B., Lin, S.J., Müller, J.F. and Thompson, A.M.: Atmospheric sulfur cycle simulated in the global model GOCART: Model description and global properties, J. Geophys. Res. Atmos, 105, 24671-24687, https://doi.org/10.1029/2000JD900384, 2000.

Crippa, M., Canonaco, F., Lanz, V. A., Äijälä, M., Allan, J. D., Carbone, S., Capes, G., Ceburnis, D., Dall'Osto, M., Day, D. A., DeCarlo, P. F., Ehn, M., Eriksson, A., Freney, E., Hildebrandt Ruiz, L., Hillamo, R., Jimenez, J. L., Junninen, H., Kiendler-Scharr, A., Kortelainen, A.-M., Kulmala, M., Laaksonen, A., Mensah, A. A., Mohr, C., Nemitz, E., O'Dowd, C., Ovadnevaite, J., Pandis, S. N., Petäjä, T., Poulain, L., Saarikoski, S., Sellegri, K., Swietlicki, E., Tiitta, P., Worsnop, D. R., Baltensperger, U., and Prévôt, A. S. H.: Organic aerosol components derived from 25 AMS data sets across Europe using a consistent ME-2 based source apportionment approach, Atmos. Chem. Phys., 14, 6159–6176, https://doi.org/10.5194/acp-14-6159-2014, 2014.

Cubison, M. J., Ortega, A. M., Hayes, P. L., Farmer, D. K., Day, D., Lechner, M. J., Brune, W. H., Apel, E., Diskin, G. S., Fisher, J. A., Fuelberg, H. E., Hecobian, A., Knapp, D. J., Mikoviny, T., Riemer, D., Sachse, G. W., Sessions, W., Weber, R. J., Weinheimer, A. J., Wisthaler, A., and Jimenez, J. L.: Effects of aging on organic aerosol from open biomass burning smoke in aircraft and laboratory studies, Atmos. Chem. Phys., 11, 12049–12064, https://doi.org/10.5194/acp-11-12049-2011, 2011.

Cubison, M. J., Ortega, A. M., Hayes, P. L., Farmer, D. K., Day, D., Lechner, M. J., Brune, W. H., Apel, E., Diskin, G. S., Fisher, J. A., Fuelberg, H. E., Hecobian, A., Knapp, D. J., Mikoviny, T., Riemer, D., Sachse, G. W., Sessions, W., Weber, R. J., Weinheimer, A. J., Wisthaler, A., and Jimenez, J. L.: Effects of aging on organic aerosol from open biomass burning smoke in aircraft and laboratory studies, Atmos. Chem. Phys., 11, 12049–12064, https://doi.org/10.5194/acp-11-12049-2011, 2011

de Gouw, J. A., Middlebrook, A. M., Warneke, C., Goldan, P. D., Kuster, W. C., Roberts, J. M., Fehsenfeld, F. C., Worsnop, D. R., Canagaratna, M. R., Pszenny, A. A. P., Keene, W. C.,Marchewka, M., Bertman, S. B., and

https://doi.org/10.5194/egusphere-2026-1302
Preprint. Discussion started: 13 March 2026

Bates, T. S.: Budget of organic carbon in a polluted atmosphere: Results from the New England air quality study in 2002, J. Geophys. Res., 110, D16305, https://doi.org/10.1029/2004JD005623 , 2005.

de Gouw, J. and Jimenez, J. L.: Organic aerosols in the earth's atmosphere, Environ. Sci. Technol., 43, 7614–7618, https://doi.org/10.1021/es9006004, 2009.

De Gouw, J.A., Brock, C.A., Atlas, E.L., Bates, T.S., Fehsenfeld, F.C., Goldan, P.D., Holloway, J.S., Kuster, W.C., Lerner, B.M., Matthew, B.M. and Middlebrook, A.M.: Sources of particulate matter in the northeastern United States in summer: 1. Direct emissions and secondary formation of organic matter in urban plumes, J. Geophys. Res. Atmos, 113, D08301, https://doi.org/10.1029/2007JD009243, 2008.

DeCarlo, P. F., Kimmel, J. R., Trimborn, A., Northway, M. J., Jayne, J. T., Aiken, A. C., Gonin, M., Fuhrer, K., Horvath, T., Docherty, K. S., Worsnop, D. R., and Jimenez, J. L.: Field-deployable, high-resolution, time-of-flight aerosol mass spectrometer, Anal. Chem., 78, 8281–8289, https://doi.org/10.1021/ac061249n , 2006.

DeCarlo, P. F., Ulbrich, I. M., Crounse, J., de Foy, B., Dunlea, E. J., Aiken, A. C., Knapp, D., Weinheimer, A. J., Campos, T., Wennberg, P. O., and Jimenez, J. L.: Investigation of the sources and processing of organic aerosol over the Central Mexican Plateau from aircraft measurements during MILAGRO, Atmos. Chem. Phys., 10, 5257–5280, https://doi.org/10.5194/acp-10-5257-2010, 2010.

DeCarlo, P. F., Ulbrich, I. M., Crounse, J., de Foy, B., Dunlea, E. J., Aiken, A. C., Knapp, D., Weinheimer, A. J., Campos, T., Wennberg, P. O., and Jimenez, J. L.: Investigation of the sources and processing of organic aerosol over the Central Mexican Plateau from aircraft measurements during MILAGRO, Atmos. Chem. Phys., 10, 5257–5280, https://doi.org/10.5194/acp-10-5257-2010, 2010.

Drosatou, A. D., Skyllakou, K., Theodoritsi, G. N., and Pandis, S. N.: Positive matrix factorization of organic aerosol: insights from a chemical transport model, Atmos. Chem. Phys., 19, 973–986, https://doi.org/10.5194/acp-19-973-2019, 2019.

Emmons, L. K., Walters, S., Hess, P. G., Lamarque, J.-F., Pfister, G. G., Fillmore, D., Granier, C., Guenther, A., Kinnison, D., Laepple, T., Orlando, J., Tie, X., Tyndall, G., Wiedinmyer, C., Baughcum, S. L., and Kloster, S.: Description and evaluation of the Model for Ozone and Related chemical Tracers, version 4 (MOZART-4), Geosci. Model Dev., 3, 43–67, https://doi.org/10.5194/gmd-3-43-2010, 2010.

Ervens, B., Turpin, B. J., and Weber, R. J.: Secondary organic aerosol formation in cloud droplets and aqueous particles (aqSOA): a review of laboratory, field and model studies, Atmos. Chem. Phys., 11, 11069–11102, https://doi.org/10.5194/acp-11-11069-2011, 2011.

Forster, P., Ramaswamy, V., Artaxo, P., Berntsen, T., Betts, R., Fahey, D. W., Haywood, J., Lean, J., Lowe, D. C., Myhre, G., Nganga, J., Prinn, R., Raga, G., Schulz, M., and Van Dorland, R.: Changes in Atmospheric Constituents and in Radiative Forcing, in: Climate Change 2007: The Physical Science Basis. Contribution of Working Group I to the Fourth Assessment Report of the Intergovernmental Panel on Climate Change., Cambridge University Press, Cambridge, United Kingdom and New York, NY, USA,2007.

Fröhlich, R., Crenn, V., Setyan, A., Belis, C. A., Canonaco, F., Favez, O., Riffault, V., Slowik, J. G., Aas, W., Aijälä, M., Alastuey, A., Artiñano, B., Bonnaire, N., Bozzetti, C., Bressi, M., Carbone, C., Coz, E., Croteau, P. L., Cubison, M. J., Esser-Gietl, J. K., Green, D. C., Gros, V., Heikkinen, L., Herrmann, H., Jayne, J. T., Lunder, C. R., Minguillón, M. C., Močnik, G., O'Dowd, C. D., Ovadnevaite, J., Petralia, E., Poulain, L., Priestman, M., Ripoll, A., Sarda-Estève, R., Wiedensohler, A., Baltensperger, U., Sciare, J., and Prévôt, A. S. H.: ACTRIS ACSM intercomparison – Part 2: Intercomparison of ME-2 organic source apportionment results from 15 individual, co-located aerosol mass spectrometers, Atmos. Meas. Tech., 8, 2555–2576, https://doi.org/10.5194/amt-8-2555-2015, 2015.

Ghude, S. D., S. Fadnavis, G. Beig, S. D. Polade, and R. J. van der A.: Detection of surface emission hot spots, trends, and seasonal cycle from satellite-retrieved NO2 over India. J. Geophys. Res., 113, D20305, https://doi.org/10.1029/2007JD009615, 2008.

https://doi.org/10.5194/egusphere-2026-1302
Preprint. Discussion started: 13 March 2026

Ghude, S.D., Kalita, G., Jat, R., Govardhan, G., Debnath, S., Yadav, P.P., Ambulkar, R., Kumar, R. and Attri, S.D.: The role of atmospheric feedback and groundwater conservation policies in degrading air quality in Delhi, npj Clean Air 1, 12 (2025). https://doi.org/10.1038/s44407-025-00012-x, 2025.

Ghude, S.D.,Govardhan, G., Kumar, R., Yadav, P.P., Jat, R., Debnath, S., Kalita, G., Jena, C., Ingle, S., Gunwani, P., Pawar, P.V., Ambulkar, R., Kumar, S., Kulkarni, S., Kulkarni, A., Khare, M., Kaginalkar, A., Soni, V.K., Nigam, N., Ray, K., Atri, S.D., Nanjundiah, R., and Rajeevan. M.: Air Quality Warning and Integrated decision Support system for Emissions (AIRWISE): Enhancing Air Quality management in Megacities. Bull. Am. Meterol. Soc., 105, E2525-E2550. https://doi.org/10.1175/BAMS-D-23-0181.1, 2024.

Ginoux, P., Chin, M., Tegen, I., Prospero, J.M., Holben, B., Dubovik, O. and Lin, S.J.: Sources and distributions of dust aerosols simulated with the GOCART model, J. Geophys. Res. Atmos., 106 ,20255-20273, https://doi.org/10.1029/2000JD000053, 2021.

Govardhan, G., Ambulkar, R., Kulkarni, S., Vishnoi, A., Yadav, P., Choudhury, B.A., Khare, M. and Ghude, S.D.: Stubble-burning activities in north-western India in 2021: Contribution to air pollution in Delhi. Heliyon, 9, 16939, https://doi.org/10.1016/j.heliyon.2023.e16939, 2023.

Grell, G.A., Peckham, S.E., Schmitz, R., McKeen, S.A., Frost, G., Skamarock, W.C. and Eder, B.: Fully coupled "online" chemistry within the WRF model, Atmos. Environ., 39, 6957-6975, https://doi.org/10.1016/j.atmosenv.2005.04.027, 2005.

Grell, G. A., and Freitas S.R.: A scale and aerosol aware stochastic convective parameterization for weather and air quality modeling. Atmos. Chem. Phys., 14, 5233–5250, https://doi.org/10.5194/acp-14-5233-2014, 2014.

Guenther, A., Karl, T., Harley, P., Wiedinmyer, C., Palmer, P. I., and Geron, C.: Estimates of global terrestrial isoprene emissions using MEGAN (Model of Emissions of Gases and Aerosols from Nature), Atmos. Chem. Phys., 6, 3181–3210, https://doi.org/10.5194/acp-6-3181-2006, 2006.

Gurjar, B. R., Ravindra , K., and Nagpure, A. S.: Air pollution trends over Indian megacities and their local-to-global implications. Atmos. Environ., 142, 475–495, https://doi.org/10.1016/j.atmosenv.2016.06.030, 2016.

Hakkim, H., Kumar, A., Annadate, S., Sinha, B. and Sinha, V.: RTEII: A new high-resolution (0.1× 0.1) road transport emission inventory for India of 74 speciated NMVOCs, CO, NOx, NH3, CH4, CO2, PM2.5 reveals massive overestimation of NOx and CO and missing nitromethane emissions by existing inventories, Atmos. Environ. X, 11, 100118, https://doi.org/10.1016/j.aeaoa.2021.100118 , 2021.

Harvey, R.M. and Petrucci, G.A.: Control of ozonolysis kinetics and aerosol yield by nuances in the molecular structure of volatile organic compounds, Atmos. Environ., 122, 188-195. https://doi.org/10.1016/j.atmosenv.2015.09.038 , 2015.

Hildebrandt, L., Donahue, N. M., and Pandis, S. N.: High formation of secondary organic aerosol from the photo-oxidation of toluene, Atmos. Chem. Phys., 9, 2973–2986, https://doi.org/10.5194/acp-9-2973-2009, 2009.

Hodzic, A. and Jimenez, J. L.: Modeling anthropogenically controlled secondary organic aerosols in a megacity: a simplified framework for global and climate models, Geosci. Model Dev., 4, 901–917, https://doi.org/10.5194/gmd-4-901-2011, 2011.

Hodzic, A., Campuzano-Jost, P., Bian, H., Chin, M., Colarco, P. R., Day, D. A., Froyd, K. D., Heinold, B., Jo, D. S., Katich, J. M., Kodros, J. K., Nault, B. A., Pierce, J. R., Ray, E., Schacht, J., Schill, G. P., Schroder, J. C., Schwarz, J. P., Sueper, D. T., Tegen, I., Tilmes, S., Tsigaridis, K., Yu, P., and Jimenez, J. L.: Characterization of organic aerosol across the global remote troposphere: a comparison of ATom measurements and global chemistry models, Atmos. Chem. Phys., 20, 4607–4635, https://doi.org/10.5194/acp-20-4607-2020, 2020.

Hodzic, A., Jimenez, J. L., Madronich, S., Canagaratna, M. R., DeCarlo, P. F., Kleinman, L., and Fast, J.: Modeling organic aerosols in a megacity: potential contribution of semi-volatile and intermediate volatility primary organic

https://doi.org/10.5194/egusphere-2026-1302
Preprint. Discussion started: 13 March 2026

compounds to secondary organic aerosol formation, Atmos. Chem. Phys., 10, 5491–5514, https://doi.org/10.5194/acp-10-5491-2010, 2010a.

Hodzic, A., Kasibhatla, P. S., Jo, D. S., Cappa, C. D., Jimenez, J. L., Madronich, S., and Park, R. J.: Rethinking the global secondary organic aerosol (SOA) budget: stronger production, faster removal, shorter lifetime, Atmos. Chem. Phys., 16, 7917–7941, https://doi.org/10.5194/acp-16-7917-2016, 2016.

Iacono, M. J., J. S. Delamere, E. J. Mlawer, M. W. Shephard, S. A. Clough, and W. D. Collins.: Radiative forcing by long-lived greenhouse gases: Calculations with the AER radiative transfer models. J. Geophys. Res., 113, D13103, https://doi.org/10.1029/2008JD009944, 2008.

Jat

Janjić, Z. I.: Nonsingular implementation of the Mellor–Yamada level 2.5 scheme in the NCEP Meso Model. NCEP Office Note 437, 61, 2001.

Janssens-Maenhout, G., Crippa, M., Guizzardi, D., Dentener, F., Muntean, M., Pouliot, G., Keating, T., Zhang, Q., Kurokawa, J., Wankmüller, R., Denier van der Gon, H., Kuenen, J. J. P., Klimont, Z., Frost, G., Darras, S., Koffi, B., and Li, M.: HTAP_v2.2: a mosaic of regional and global emission grid maps for 2008 and 2010 to study hemispheric transport of air pollution, Atmos. Chem. Phys., 15, 11411–11432, https://doi.org/10.5194/acp-15-11411-2015, 2015.

Jat, R., Ghude, S.D., Govardhan, G., Kumar, R., Yadav, P.P., Sharma, P., Kalita, G., Debnath, S., Kulkarni, S.H., Chate, D.M. and Nanjundiah, R.S.: Effectiveness of respiratory face masks in reducing acute PM2. 5 pollution exposure during peak pollution period in Delhi. Sci. Total Environ., *943*, 173787, https://doi.org/10.1016/j.scitotenv.2024.173787, 2024.

Jat, R., Gurjar, B.R. and Lowe, D.: Regional pollution loading in winter months over India using high resolution WRF-Chem simulation. Atmos. Res., 249, 105326, https://doi.org/10.1016/j.atmosres.2020.105326, 2021.

Jat, R., Vispute, A. S., Ghude, S. D., Kumar, R., Sinha, V., Sinha, B., Govardhan, G., Tao, Z., Yadav, P. P., Wagh, S., Debnath, S., Rathore, A., and Rajeevan, M.: Code and data for: Implementation and Evaluation of an Observation-Constrained Secondary Organic Aerosol Parameterization in MOZART–GOCART Chemistry in WRF-Chem (v1.0), Zenodo, https://doi.org/10.5281/zenodo.18937872, 2026.

Jena, C., Ghude, S.D., Kumar, R., Debnath, S., Govardhan, G., Soni, V.K., Kulkarni, S.H., Beig, G., Nanjundiah, R.S. and Rajeevan, M.: Performance of high resolution (400 m) PM2. 5 forecast over Delhi, Sci. Rep., 11, 4104, https://doi.org/10.1038/s41598-021-83467-8, 2021.

Knote, C., Hodzic, A., and Jimenez, J. L.: The effect of dry and wet deposition of condensable vapors on secondary organic aerosols concentrations over the continental US, Atmos. Chem. Phys., 15, 1–18, https://doi.org/10.5194/acp-15-1-2015, 2015.

Kumar R., Meech, S., Yadav, P.P., Cheng, W., Ghude, S.D., Alessandrini, S., Jat, R. and Govardhan, G.: Will assimilating VIIRS AOD data improve New Delhi's air pollution forecasts as much as assimilating MODIS AOD?, Atmos. Environ., 121526, https://doi.org/10.1016/j.atmosenv.2025.121526, 2025

Kumar, A., Hakkim, H., Sinha, B., and Sinha, V.: Gridded 1 km × 1 km emission inventory for paddy stubble 75 burning emissions over north-west India constrained by measured emission factors of 77 VOCs and districtwise crop yield data, Sci. Total. Environ., 789, 148064, https://doi.org/10.1016/J.SCITOTENV.2021.148064 , 2021.

Kumar, P., Khare, M., Harrison, R. M., Bloss, W. J., Lewis, A. Coe, C. H. and Morawska, L.: New directions: Air pollution challenges for developing megacities like Delhi. Atmos. Environ., 122, 657–661, https://doi.org/10.1016/j.atmosenv.2015.10.032, 2015.

Kumar, R., Ghude, S.D., Biswas, M., Jena, C., Alessandrini, S., Debnath, S., Kulkarni, S., Sperati, S., Soni, V.K., Nanjundiah, R.S. and Rajeevan, M.: Enhancing accuracy of air quality and temperature forecasts during paddy

https://doi.org/10.5194/egusphere-2026-1302
Preprint. Discussion started: 13 March 2026

crop residue burning season in Delhi via chemical data assimilation, J. Geophys. Res. Atmos., 125, e2020JD033019. https://doi.org/10.1029/2020JD033019, 2020.

Lannuque, V., Camredon, M., Couvidat, F., Hodzic, A., Valorso, R., Madronich, S., Bessagnet, B., and Aumont, B.: Exploration of the influence of environmental conditions on secondary organic aerosol formation and organic species properties using explicit simulations: development of the VBS-GECKO parameterization, Atmos. Chem. Phys., 18, 13411–13428, https://doi.org/10.5194/acp-18-13411-2018, 2018.

Mishra, S., Sinha, V., Hakkim, H., Awasthi, A., Ghude, S. D., Soni, V. K., Nigam, N., Sinha, B., and Rajeevan, M. N.: Reactive chlorine-, sulfur-, and nitrogen-containing volatile organic compounds impact atmospheric chemistry in the megacity of Delhi during both clean and extremely polluted seasons, Atmos. Chem. Phys., 24, 13129–13150, https://doi.org/10.5194/acp-24-13129-2024, 2024.

Morrison, H., G. Thompson, and V. Tatarskii.: Impact of cloud microphysics on the development of trailing stratiform precipitation in a simulated squall line: Comparison of one- and two-moment schemes. Mon. Wea. Rev., **137**, 991–1007, https://doi.org/10.1175/2008MWR2556.1, 2009.

Nakanishi, M., and H. Niino.: An improved Mellor–Yamada level-3 model: Its numerical stability and application to a regional prediction of advection fog. Bound.-Layer Meteor., 119, 397–407, https://doi.org/10.1007/s10546-005-9030-8, 2006.

Ng, N. L., Kroll, J. H., Chan, A. W. H., Chhabra, P. S., Flagan, R. C., and Seinfeld, J. H.: Secondary organic aerosol formation from m-xylene, toluene, and benzene, Atmos. Chem. Phys., 7, 3909–3922, https://doi.org/10.5194/acp-7-3909-2007, 2007.

Oak, Y.J., Park, R.J., Jo, D.S., Hodzic, A., Jimenez, J.L., Campuzano-Jost, P., Nault, B.A., Kim, H., Kim, H., Ha, E.S. and Song, C.K.: Evaluation of secondary organic aerosol (SOA) simulations for Seoul, Korea, J. Adv. Model. Earth Syst., 14, e2021MS002760, https://doi.org/10.1029/2021MS002760, 2022.

Pandey, A., Brauer, M., Cropper, M.L., Balakrishnan, K., Mathur, P., Dey, S., Turkgulu, B., Kumar, G.A., Khare, M., Beig, G., Gupta, T., Krishnankutty, R.P., Causey, K., Cohen, A.J., Bhargava, S., Aggarwal, A.N., Agrawal, A., Awasthi, S., Bennitt, F., Bhagwat, S., and Dandona, L.: Health and economic impact of air pollution in the states of India: the Global Burden of Disease Study 2019, Lancet Planetary Health, 5, e25–e38, https://doi.org/10.1016/S2542-5196(20)30298-9, 2021.

Pankow, J.F.: An absorption model of the gas/aerosol partitioning involved in the formation of secondary organic aerosol, Atmos. Environ., 28, 189-193, https://doi.org/10.1016/j.atmosenv.2007.10.060, 1994.

Ramasamy, S., Nakayama, T., Imamura, T., Morino, Y., Kajii, Y. and Sato, K.: Investigation of dark condition nitrate radical-and ozone-initiated aging of toluene secondary organic aerosol: Importance of nitrate radical reactions with phenolic products, Atmos. Environ., 219, 117049. https://doi.org/10.1016/j.atmosenv.2019.117049, 2019.

Robinson, A.L., Donahue, N.M., Shrivastava, M.K., Weitkamp, E.A., Sage, A.M., Grieshop, A.P., Lane, T.E., Pierce, J.R. and Pandis, S.N.: Rethinking organic aerosols: Semivolatile emissions and photochemical aging. *Science*, 315, 1259-1262. https://doi.org/10.1126/science.1133061, 2007.

Sasidharan, S., He, Y., Akherati, A., Li, Q., Li, W., Cocker, D., McDonald, B.C., Coggon, M.M., Seltzer, K.M., Pye, H.O., Pierce, J.R., and Jathar, S.H.: Secondary organic aerosol formation from volatile chemical product emissions: Model parameters and contributions to anthropogenic aerosol, Environ. Sci. Technol., 57, 11891-11902. https://doi.org/10.1021/acs.est.3c00683, 2023.

Schell, B., Ackermann, I.J., Hass, H., Binkowski, F.S., and Ebel, A.: Modeling the formation of secondary organic aerosol within a comprehensive air quality model system, J. Geophys. Res. Atmos., 106, 28275–28293. https://doi.org/10.1029/2001JD000384 , 2001.

https://doi.org/10.5194/egusphere-2026-1302
Preprint. Discussion started: 13 March 2026

Sengupta, A., Govardhan, G., Debnath, S., Yadav, P., Kulkarni, S.H., Parde, A.N., Lonkar, P., Dhangar, N., Gunwani, P., Wagh, S. and Nivdange, S.: Probing into the wintertime meteorology and particulate matter (PM2. 5 and PM10) forecast over Delhi, Atmos. Pollut. Res., *13*, 101426. https://doi.org/10.1016/j.apr.2022.101426 , 2022.

Shrivastava, M., Fast, J., Easter, R., Gustafson Jr., W. I., Zaveri, R. A., Jimenez, J. L., Saide, P., and Hodzic, A.: Modeling organic aerosols in a megacity: comparison of simple and complex representations of the volatility basis set approach, Atmos. Chem. Phys., 11, 6639–6662, https://doi.org/10.5194/acp-11-6639-2011, 2011.

Spracklen, D. V., Jimenez, J. L., Carslaw, K. S., Worsnop, D. R., Evans, M. J., Mann, G. W., Zhang, Q., Canagaratna, M. R., Allan, J., Coe, H., McFiggans, G., Rap, A., and Forster, P.: Aerosol mass spectrometer constraint on the global secondary organic aerosol budget, Atmos. Chem. Phys., 11, 12109–12136, https://doi.org/10.5194/acp-11-12109-2011, 2011.

Stockwell, W.R., Middleton, P., Chang, J.S., and Tang, X.: The second generation regional acid deposition model chemical mechanism for regional air quality modeling. J. Geophys. Res. 95, 16343–16367, https://doi.org/10.1029/JD095iD10p16343, 1990.

Tsimpidi, A. P., Karydis, V. A., Pandis, S. N., and Lelieveld, J.: Global combustion sources of organic aerosols: model comparison with 84 AMS factor-analysis data sets, Atmos. Chem. Phys., 16, 8939–8962, https://doi.org/10.5194/acp-16-8939-2016 , 2016.

Ulbrich, I. M., Canagaratna, M. R., Zhang, Q., Worsnop, D. R., and Jimenez, J. L.: Interpretation of organic components from Positive Matrix Factorization of aerosol mass spectrometric data, Atmos. Chem. Phys., 9, 2891–2918, https://doi.org/10.5194/acp-9-2891-2009, 2009.

Venkataraman, C., Brauer, M., Tibrewal, K., Sadavarte, P., Ma, Q., Cohen, A., Chaliyakunnel, S., Frostad, J., Klimont, Z., Martin, R. V., Millet, D. B., Philip, S., Walker, K., and Wang, S.: Source influence on emission pathways and ambient PM2.5 pollution over India (2015–2050), Atmos. Chem. Phys., 18, 8017–8039, https://doi.org/10.5194/acp-18-8017-2018, 2018.

Vispute, A.S., Acharja, P., Gosavi, S.W., Govardhan, G., Ruge, V., Patil, M.N., Dharmaraj, T. and Ghude, S.D.: Source characteristics of non-refractory particulate matter (NR-PM1) using high-resolution time-of-flight aerosol mass spectrometric (HR-ToF-AMS) measurements in the urban industrial city in India. Atmos. Environ., *351*, 121186, https://doi.org/10.1016/j.atmosenv.2025.121186, 2025.

Wiedinmyer, C., Kimura, Y., McDonald-Buller, E. C., Emmons, L. K., Buchholz, R. R., Tang, W., Seto, K., Joseph, M. B., Barsanti, K. C., Carlton, A. G., and Yokelson, R.: The Fire Inventory from NCAR version 2.5: an updated global fire emissions model for climate and chemistry applications, Geosci. Model Dev., 16, 3873–3891, https://doi.org/10.5194/gmd-16-3873-2023, 2023.

Yadav, P.P., Ghude, S.D., Kumar, R., Govardhan, G., Jat, R., Shah, S., Shukla, B.P., Mishra, M.K., Putrevu, D., Thapliyal, P.K. and Sharma, R.: Assimilation of high-resolution Ocean Color Monitor (OCM) aerosol optical depth in WRF-Chem improves $PM_{2.5}$ forecasts over the Indian region, Sci. Rep., 15, 39669. https://doi.org/10.1038/s41598-025-23307-1, 2025b.

Yadav, P.P., Jat, R., Ghude, S.D., Govardhan, G., Kumar, R., Debnath, S., Kalita, G., Jena, C., Soni, V.K., Jayakumar, A., Anurose, T.J., Bhati, S., Sayeed, A., Seo, J., Gupta, P., Bhattacharjee, P.S., Flemming, J., Ray, K. and Atri, S.D.: Evaluating the performance of regional and global forecasting models for accurate PM2. 5 prediction and air quality index assessment in Delhi, India, J. Geophys. Res. Atmos., 130, e2025JD043719, https://doi.org/10.1029/2025JD043719 , 2025a.

Zaveri, R.A., Easter, R.C., Fast, J.D., and Peters, L.K.: Model for Simulating Aerosol Interactions and Chemistry (MOSAIC), J. Geophys. Res. Atmos., 113, 1–29. https://doi.org/10.1029/2007JD008782, 2008.

https://doi.org/10.5194/egusphere-2026-1302
Preprint. Discussion started: 13 March 2026

Zhang, Q., Sarkar, S., Wang, X., Zhang, J., Mao, J., Yang, L., Shi, Y., and Jia, S.: Evaluation of factors influencing secondary organic carbon (SOC) estimation by CO and EC tracer methods, Sci. Total Environ., 686, 915-930, https://doi.org/10.1016/j.scitotenv.2019.05.402, 2019.